

Observation of fission in Pb-Pb interactions at 158A GeV

M. C. Abreu,^{6,*} B. Alessandro,¹¹ C. Alexa,³ R. Arnaldi,¹¹ J. Astruc,⁸ M. Atayan,¹³ C. Baglin,¹ A. Baldit,² L. Bardi,¹¹ M. Bedjidian,¹² F. Bellaiche,¹² S. Beolè,¹¹ V. Boldea,³ P. Bordalo,^{6,†} A. Bussière,¹ L. Casagrande,⁶ J. Castor,² T. Chambon,² B. Chaurand,⁹ I. Chevrot,² B. Cheynis,¹² E. Chiavassa,¹¹ C. Cicalò,⁴ M. P. Comets,⁸ S. Constantinescu,³ P. Cortese,¹¹ J. Cruz,⁶ A. DeFalco,⁴ N. DeMarco,¹¹ G. Dellacasa,^{11,‡} A. Devaux,² S. Dita,³ O. Drapier,¹² B. Espagnon,² J. Fargeix,² F. Fleuret,^{9,§} P. Force,² M. Gallio,¹¹ Y. K. Gavrilo, ⁷ C. Gerschel,⁸ P. Giubellino,¹¹ M. B. Golubeva,⁷ M. Gonin,⁹ A. A. Grigorian,¹³ J. Y. Grossiord,¹² F. F. Guber,⁷ A. Guichard,¹² H. Gulkanyan,¹³ R. Hakobyan,¹³ R. Haroutunian,¹² M. Idzik,^{11,||} D. Jouan,⁸ T. L. Karavitcheva,⁷ L. Klumberg,⁹ A. B. Kurepin,⁷ G. Landaud,² Y. LeBornec,⁸ C. Lourenço,⁵ L. Luquin,² M. MacCormick,⁸ M. P. Macciotta,⁴ A. Marzari-Chiesa,¹¹ M. Masera,¹¹ A. Masoni,⁴ S. Mehrabyan,¹³ M. Monteno,¹¹ S. Mourgues,² A. Musso,¹¹ F. Ohlsson-Malek,^{12,¶} P. Petiau,⁹ A. Piccotti,¹¹ J. R. Pizzi,¹² W. Prado da Silva,^{11,**} G. Puddu,⁴ C. Quintans,⁶ C. Racca,¹⁰ L. Ramello,^{11,‡} S. Ramos,^{6,†} P. Rato-Mendes,¹¹ L. Riccati,¹¹ A. Romana,⁹ I. Ropotar,^{5,††} P. Saturnini,² E. Scomparin,^{5,‡‡} S. Serci,⁴ R. Shahoyan,^{6,§§} S. Silva,⁶ M. Sitta,^{11,‡} C. Soave,¹¹ P. Sonderegger,^{5,†} X. Tarrago,⁸ N. S. Topilskaya,⁷ G. L. Usai,⁴ C. Vale,⁶ E. Vercellin,¹¹ and N. Willis⁸

(NA50 Collaboration)

¹Laboratoire de Physique des Particules (LAPP), CNRS-IN2P3, Annecy-le-Vieux, France

²Laboratoire de Physique Corpusculaire, Université Blaise Pascal, Aubière, France
and CNRS-IN2P3, Aubière, France

³Institute of Atomic Physics (IFA), Bucharest, Romania

⁴Università di Cagliari/INFN, Cagliari, Italy

⁵CERN, Geneva, Switzerland

⁶Laboratório de Instrumentação e Física Experimental de Partículas (LIP), Lisbon, Portugal

⁷Institute for Nuclear Research (INR), Moscow, Russia

⁸Institut de Physique Nucléaire (IPN), Université de Paris-Sud, Orsay, France
and CNRS-IN2P3, Orsay, France

⁹Laboratoire de Physique Nucléaire des Hautes Energies (LPNHE), Ecole Polytechnique, Palaiseau, France
and CNRS-IN2P3, Palaiseau, France

¹⁰Institut de Recherches Subatomiques (IReS), Université Louis Pasteur, Strasbourg, France
and CNRS-IN2P3, Strasbourg, France

¹¹Università di Torino/INFN, Torino, Italy

¹²Institut de Physique Nucléaire de Lyon (IPN), Université Claude Bernard, Villeurbanne, France
and CNRS-IN2P3, Villeurbanne, France

¹³YerPhI, Yerevan, Armenia

(Received 22 July 1998)

The NA50 experiment at the CERN SPS has been equipped with a Cerenkov quartz detector to measure the charge of projectilelike fragments emitted in interactions of the lead beam of 158A GeV with a 12 mm thick lead target. A clear fission peak has been observed in the light output distribution of the fragment detector and the measured number of fission events per incident Pb ion is $(1.26 \pm 0.16) \times 10^{-2}$. The information provided by the NA50 zero-degree calorimeter has allowed us to check that fission occurs in extremely peripheral collisions. To provide the first information about the fission mechanism, the expected yield of electromagnetic fission events in our experimental conditions has been computed: it turns out to be about 40% smaller than the observed one. The approximations necessarily made in our calculation as well as the contribution due to fission induced by nuclear interaction could account for such a difference. [S0556-2813(99)05501-6]

PACS number(s): 25.75.-q, 25.70.Mn, 25.85.Ge

*Also at FCUL, Universidade de Lisboa, Lisbon, Portugal.

†Also at IST, Universidade Tecnica de Lisboa, Lisbon, Portugal.

‡Also at Dipartimento di Scienze e Tecnologie Avanzate, II Facoltà di Scienze, Alessandria, Italy.

§Now at LPNHE, University PARIS VI-VII, Paris, France.

||Now at Faculty of Physics and Nuclear Techniques, University of Mining and Metallurgy, Cracow, Poland.

¶Now at ISN, Université Joseph Fourier and CNRS-IN2P3, Grenoble, France.

**Now at UERJ, Rio de Janeiro, Brazil.

††Also at Bergische-Universität Gesamthochschule, Wuppertal, Germany.

‡‡On leave of absence from INFN, Torino, Italy.

§§On leave of absence from YerPhI, Yerevan, Armenia.

I. INTRODUCTION

In heavy-ion collisions fission can be induced both by nuclear and electromagnetic interaction. Roughly speaking, the former mechanism is dominant for collisions where the minimum distance between the centers of the colliding nuclei is smaller than the sum of the nuclear radii. On the other hand only the latter mechanism plays a role when the minimum distance is larger than the sum of the radii. This case is often referred to as electromagnetic fission or Coulomb fission [1–3].

Fission of ^{238}U projectiles interacting on different nuclear targets has been recently studied at relativistic energies, between 120A MeV and 1A GeV [4–7]. According to their different target dependence, the contributions to the total fission cross section due respectively to the nuclear and to the electromagnetic excitation mechanisms can be deduced from the experimental data. In fact, as a first approximation, the cross section for the former process scales as $A_{\text{tar}}^{1/3}$ [6], while for the latter as Z_{tar}^2 (see Sec. IV A). At 1A GeV, the nuclear excitation mechanism is dominant on light targets, while on heavy ones the two contributions are comparable and a value of about 1.6 b for the Coulomb fission cross sections of ^{238}U on gold target was found [6]. Such a value is in substantial agreement with the theoretical calculations [8,3] based on the Weizsacker-Williams equivalent photon method [9,10]. Since the energy of the virtual photons increases with the bombarding energy, the electromagnetic fission cross sections become even larger in the ultra-relativistic regime. For instance for ^{238}U -Au interactions at 160A GeV the Coulomb fission cross section of uranium is expected to be about 10 b [3].

The situation is different for nuclei lighter than uranium, such as Au, Pb, Bi. Here fission occurs at higher excitation energies [11–19], so that the fission cross sections for these nuclei are much smaller compared to uranium. For instance, at bombarding energies close to 1A GeV, no influence of fission on the fragmentation of ^{208}Pb projectiles has been observed [20] and for ^{197}Au the fission cross section is only 5% of the total one [21–23]. Indeed, experiments with the AGS gold beam have found that at 10.6A GeV the fission probability of ^{197}Au is at least one order of magnitude smaller than at 1A GeV [24,25]. As it has been pointed out [24], this seems to suggest that as the energy of the projectile increases, the probability decreases for soft nuclear interactions leading to fission. Moreover, we have to note that a recent experiment at the SPS [26] studied interactions of ^{208}Pb on emulsion and “an insignificant number of fission events was observed.” This indicates that the cross section for Coulomb fission of ^{208}Pb on a light target is still small even at SPS energies.

In this paper we report an experimental study, carried out in the frame of the NA50 experiment, where projectile fission in Pb-Pb interactions at 158A GeV has been observed, although the experimental conditions were not optimized for this measurement and the fission cross section is however small, of the order of few hundreds mb.

The paper is organized as follows. The apparatus is described in Sec. II while the experimental results are presented in Sec. III. To give a first idea of the fission mechanism (nuclear vs e.m. interaction), we compute the yield of Cou-

lomb fission events expected in our experimental conditions; this calculation is reported in Sec. IV. Some conclusions are drawn in Sec. V, where further measurements that could shed more light on the fission mechanism are also briefly discussed.

II. THE EXPERIMENTAL APPARATUS

The main aim of the NA50 experiment at CERN SPS is the study of J/ψ and ψ' suppression as a signal of quark-gluon plasma formation [27] in Pb-Pb interactions at 158A GeV. A detailed description of the standard NA50 apparatus can be found in Ref. [28], and references therein. Here we simply recall that vector mesons are detected via their $\mu^+\mu^-$ decay, by measuring the invariant mass of the muon pair. The ^{208}Pb beam is counted by a quartz hodoscope and impinges on a segmented lead target (12 mm thick) [29] that is followed by a hadron absorber where the beam as well as the hadrons produced in the interaction are stopped. The absorber is crossed by the muons that are detected by the muon spectrometer which is based on an air-core toroidal magnet equipped with hexagonal multiwire proportional chambers and scintillator hodoscopes. The spectrometer covers the pseudorapidity interval $2.8 \leq \eta \leq 4.0$. Since the J/ψ and ψ' suppression is strongly related to the centrality of the collision, special care has been taken to measure the impact parameter b . For this purpose the experiment makes use of three centrality detectors: an electromagnetic calorimeter (EC), that measures the neutral transverse energy in the pseudorapidity region $1.1 \leq \eta \leq 2.3$, a silicon microstrip multiplicity detector (MD) [30] that covers the interval $1.5 \leq \eta \leq 3.9$, and a zero-degree calorimeter (ZDC), that measures the energy carried out from the Pb-Pb interaction by the projectile spectators [31,32]. As it can be seen in Fig. 1, where the target area is shown, the ZDC is placed on the beam trajectory inside the hadron absorber. To minimize the background due to particles produced in the collision, its angular acceptance ($\eta \geq 6.3$) is defined by a copper collimator with conical aperture.

For the measurements reported here a *new* detector has been added to the NA50 apparatus to provide some information on the charge of spectator fragments emitted in the decay of the Pb projectile after its interaction in the target. This measurement has been carried out in parallel to the standard NA50 data taking, i.e., in experimental conditions that are optimized for charmonium detection rather than for a fragmentation study. This consideration has driven the choice and the design of the fragment detector, that must have a small size since the only place available is inside the hadron absorber, just in front of the ZDC, as shown in Fig. 1. Moreover the detector has to be operated at the high beam intensities used in NA50 (10^7 Pb ions/sec), implying fast signals to minimize pile-up effects and high radiation hardness (several Grad). All these requirements are fulfilled by a quartz Cerenkov detector whose structure is shown in Fig. 2.

The fragment detector consists of a blade made of SiO_2 suprasil, shaped as a truncated pyramid 2 mm thick. The trajectory of the beam and of the nuclear fragments is orthogonal to the pyramid bases (about 20×20 mm² in area). The Cerenkov photons are totally reflected on both bases and exit through the side faces of the truncated pyramid that form

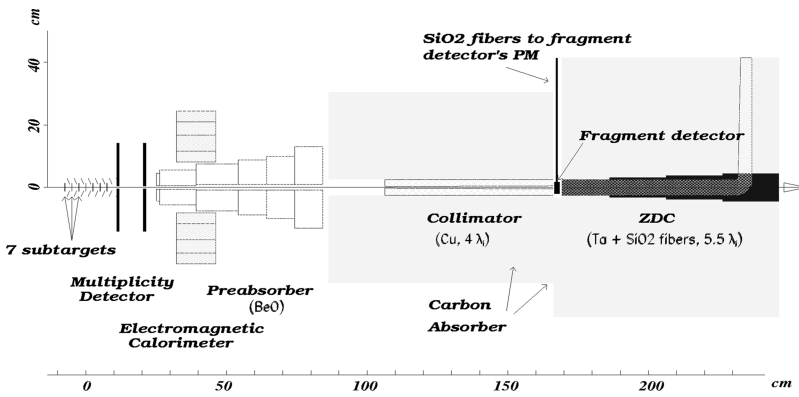


FIG. 1. Experimental layout: the fragment detector and the standard NA50 detectors in the target and hadron absorber region are shown.

an angle $\delta=47^\circ$ with respect to the beam axis. The light exiting from one of the four side faces is guided to a photomultiplier (Philips XP 2242, 6 stages) by means of quartz optical fibres (Spec-Tran HCG-M-365-U) about 80 cm long.

A simulation of the fragment detector shows that the contribution to the resolution due to photoelectron statistics is about 2.5% for Pb ions. This has to be regarded as a lower limit since photon absorption in the quartz blade and in the fibers was not taken into account. As for the ZDC, the angular acceptance of the fragment detector is determined by the collimator that has an angular aperture of 3.3 mrad, corresponding to a 7 mm radius hole on the detector front face. The simulation shows that inside this central region of the detector, its response is constant within 1%. The aperture of the collimator is large enough to ensure the detection of pro-

jectile spectators, including the fission fragments (these last are emitted at angles smaller than 1 mrad with respect to the beam axis). Therefore, since the yield of Cerenkov light is proportional to the squared charge of the particle, the quantity measured by our fragment detector is $\sum(Z_i)^2$, where Z_i is the charge of the i th fragment emitted in the decay of the projectile.

The signal of the quartz blade photomultiplier (duration 12 ns) is amplified by a factor of 40, then sent to a linear gate module and finally integrated by an ADC. The information provided by the fragment detector, together with those coming from the other detectors of the experiment, are read out and recorded by the general acquisition system. This last is enabled by the standard NA50 trigger, which is a mixture of different signals. In addition to the dimuon trigger, a small fraction of other trigger signals is in fact recorded for monitoring purposes. Among these, the one obtained by discriminating with a low threshold the zero-degree calorimeter signal (downscaled by a large factor) represents a convenient tool to collect a sample of events including peripheral collisions and uninteracting Pb ions [31]. Therefore only this trigger, selected by software, is used for the present analysis.

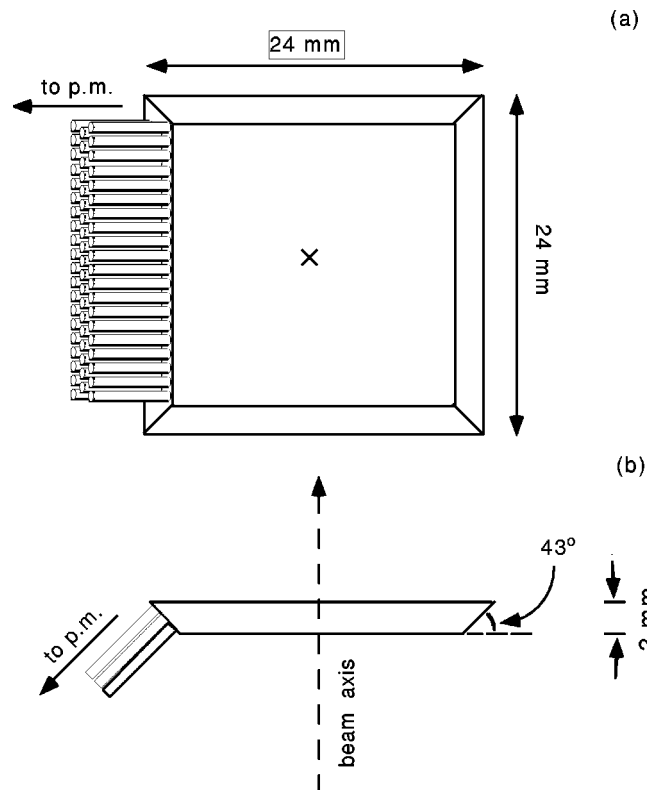


FIG. 2. Structure of the fragment detector. (a) Front view (the beam enters into the drawing); (b) top view. Note that for the sake of a clear presentation only a sample of the quartz fibers is shown and the fiber diameter is not in scale with respect to the quartz blade.

III. EXPERIMENTAL RESULTS

When placed on the beam, the fragment detector has shown a stable behavior (i.e., the amplitude of the signal due to Pb ions noninteracting in the target was found to be constant) for about five days; all the data presented here have been collected during that period of time. Then, a sudden degradation of the signal has been observed. At the end of the NA50 run the detector was dismantled and its central part, corresponding to the beam spot, has been found to be spoiled. For comparison purposes, it would have been useful to collect data without the Pb target. Unfortunately, this has not been possible during the period in which the fragment detector was in operation.

In Fig. 3(a) is shown the ADC spectrum of the fragment detector after subtraction of the pedestal and rejection of pile-up. This has been done exploiting the information of the beam quartz hodoscope and of the ZDC, according to a procedure reported in previous papers [28,31]. A first peak, centred at channel 800, is clearly visible; it corresponds to the uninteracting beam. Indeed this peak is also populated by events in which the incoming Pb ions have lost one or more neutrons, mainly by electromagnetic interactions (see Sec.

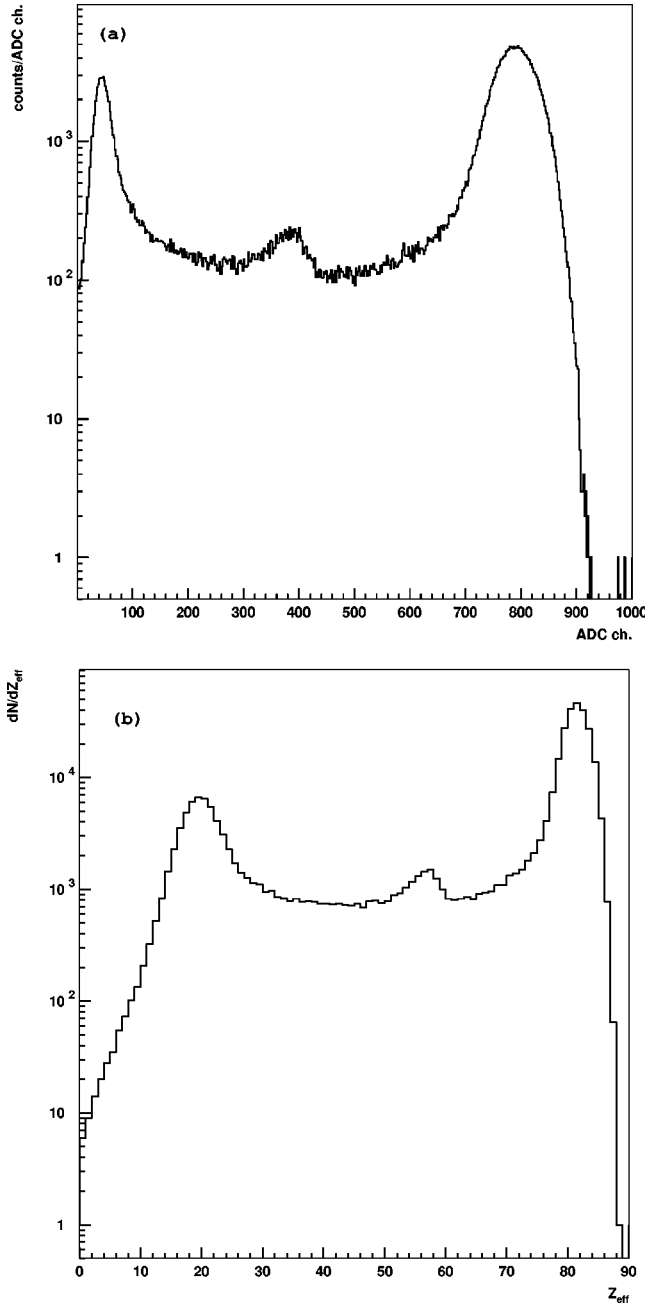


FIG. 3. (a) Light output (ADC channels) and (b) Z_{eff} spectra measured by the fragment detector. The variable Z_{eff} is defined in the text.

IV B). The relative width of the peak is about 4% r.m.s., a value that is basically in agreement with the predictions of the simulation. The number of events in the peak is about 70% of the total sample, as expected for our target thickness that corresponds to 30% of the nuclear interaction length for Pb projectiles in a Pb target.

In the same figure, a peak which is centred at channel 50 is also visible. It can be ascribed to rather central collisions where the excitation energy is high enough to multifragment the spectator system. The region between these two peaks is populated by an almost flat continuum, on top of which stands a third peak at channel 400, i.e., at one half of the Pb peak. This can be interpreted as a signal of symmetric (or quasymmetric) binary fission. In this case, in fact, a con-

centration of events is expected at $\Sigma(Z_i)^2 = 2(Z_{\text{Pb}/2})^2 = (Z_{\text{Pb}})^2/2$. We define the relative yield of fission events as the ratio n_f/n_0 between the number of events in the fission peak and the total number of events in the spectrum (i.e., the number of incident Pb ions). It turns out to be $n_f/n_0 = (1.26 \pm 0.16) \times 10^{-2}$, where the error is mainly due to the uncertainty in the extrapolation of the continuum under the fission peak, since fits with different functions lead to slightly different results. To conclude the discussion concerning Fig. 3(a), we note that our spectrum is remarkably similar to the one found in an experiment [5] where fission of uranium projectiles at 1A GeV was observed.

The response of the fragment detector can be expressed in terms of the effective charge Z_{eff} [5]. Since at constant velocity the yield of Cerenkov light is proportional to Z^2 , the square root of the light yield is proportional to the charge of the fragment. We define the effective charge Z_{eff} as the square root of the light output (i.e., of the ADC channel) normalized in such a way that the value obtained for the beam is $Z_{\text{eff}} = 82$. In general the value of Z_{eff} is close to the charge of the heaviest projectile fragment emitted in the collision. If two (or more) heavy fragments of similar charge are produced, Z_{eff} is sensitive to the charge of these fragments. For symmetric binary fission of lead we have $Z_{\text{eff}} = \sqrt{(82^2)/2} \approx 58$. The position of the fission peak is indeed very close to this value, as it can be seen in Fig. 3(b), where the distribution of Z_{eff} is shown. However it is interesting to note that the fission peak is slightly asymmetric. The tail towards low values of Z_{eff} indicates that events in which the sum of the charges of the two fragments is smaller than 82 are present in our sample. This can be due to fission accompanied by the emission of light charged particles, as well as to fission of nuclei lighter than lead (see Sec. IV B).

Let us consider the information provided by the multiplicity detector (MD). It measures the number of charged hadrons emitted in nuclear Pb-Pb interactions, but it is also sensitive to δ rays produced in the segmented target by the incoming ions. In very peripheral collisions the number of δ rays is larger than the number of hadrons, so that for these specific events the MD basically counts the number of δ rays. This number, that is proportional to $\Sigma(Z_i)^2$, can be computed for symmetric fission, assuming that in average fission occurs at about one half of the total target thickness. In this hypothesis $\Sigma(Z_i)^2$ is respectively equal to $(Z_{\text{Pb}})^2$ and to $1/2(Z_{\text{Pb}})^2$ in the first and second half of the target and its mean value is $3/4(Z_{\text{Pb}})^2$. Therefore we expect $N_{(\text{fiss})}^{\delta} \approx 3/4 N_{(\text{Pb})}^{\delta}$, where $N_{(\text{fiss})}^{\delta}$ and $N_{(\text{Pb})}^{\delta}$ are, respectively, the numbers of δ rays due to fission events and to uninteracting Pb ions. As it can be seen in the contour plot shown in Fig. 4, where the mean multiplicity measured by the different MD sectors and the effective charge are respectively represented on the vertical and horizontal axis, the data turn out to be in substantial agreement with this prediction. In fact, while for Pb ions ($Z_{\text{eff}} = 82$) the mean multiplicity is about 10, it is only about 8 for fission events ($Z_{\text{eff}} = 58$). This suggests that most of the interactions take place in the target, since in case of fission occurring upstream or downstream from the target, a number of δ rays, respectively, close to $1/2 N_{(\text{Pb})}^{\delta}$ and to $N_{(\text{Pb})}^{\delta}$ is expected.

For a better understanding of the different components

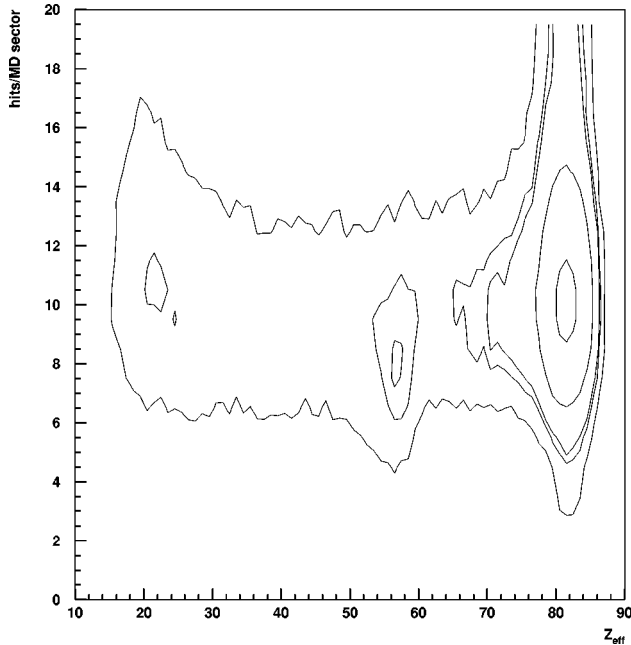


FIG. 4. Contour plot of the number of hits per multiplicity detector sector (y axis) versus Z_{eff} (x axis).

that populate the Z_{eff} spectrum, we are led to consider the information provided by the ZDC. This detector measures the zero-degree energy E_{ZDC} , i.e., the energy emitted in the very forward direction with respect to the beam. Participant nucleons undergo one or more N-N collisions and lose a significant fraction of their energy or are scattered outside the acceptance of the ZDC. Therefore, they do not contribute to E_{ZDC} , which is determined by the number of spectator nucleons. These emerge from the reaction almost unperturbed, whether as free nucleons or arranged in nuclear fragments, with in average the same energy per nucleon than that of the beam. Since the number of spectators is strongly related to the impact parameter b (small b correspond to small values of E_{ZDC}), the centrality of the collision can be deduced by measuring E_{ZDC} .

The mean value of the zero-degree energy ($\langle E_{\text{ZDC}} \rangle$) measured by the ZDC is plotted in Fig. 5 versus Z_{eff} . In view of discussing this figure, we recall that, as it can be seen in Fig. 3(b), the fission peak lies in the region $50 \leq Z_{\text{eff}} \leq 62$, on top of an almost flat continuum that spans the interval $35 \leq Z_{\text{eff}} \leq 70$, between the Pb peak and the one corresponding to central collisions. Figure 5 shows that outside the fission region, $\langle E_{\text{ZDC}} \rangle$ increases monotonically with Z_{eff} . This suggests that the continuum is mainly due to nuclear interactions, in which lighter fragments (smaller values of Z_{eff}) are more likely emitted when the impact parameter decreases (smaller values of E_{ZDC}). In Fig. 5 is also clearly visible the deviation from the behavior of the continuum that occurs in correspondence of fission events, where $\langle E_{\text{ZDC}} \rangle$ shows a sudden bump. This means that the continuum is due to collisions that are less peripheral than those leading to fission. For these last events $\langle E_{\text{ZDC}} \rangle$ reaches a value that is very close to the one of non-interacting Pb ions ($\langle E_{\text{ZDC}} \rangle = 33$ TeV, $Z_{\text{eff}} = 82$). As a first guess, the zero-degree energies for uninteracting beam and for fission events are expected to be equal in case of electromagnetic fission. On the

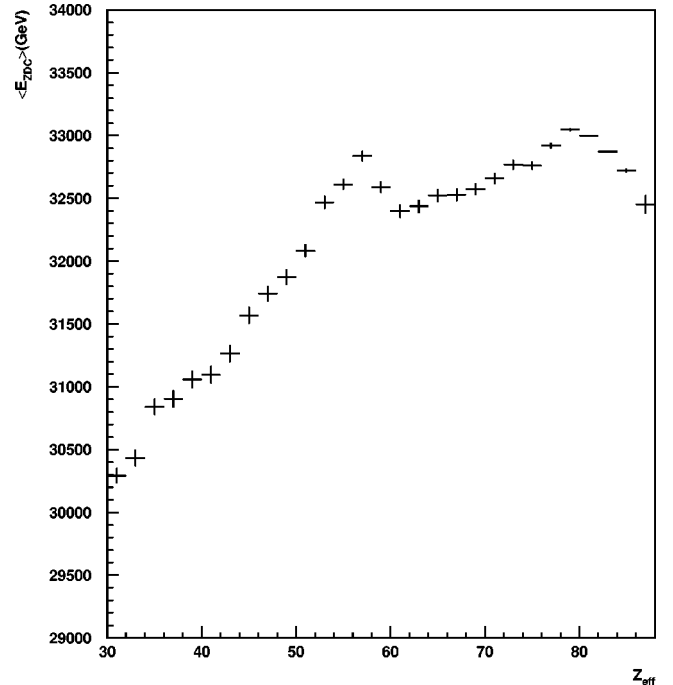


FIG. 5. Mean value of the zero-degree energy ($\langle E_{\text{ZDC}} \rangle$) per bin of Z_{eff} , plotted as a function of Z_{eff} .

other hand, for fission induced by nuclear collisions, a few (at least one) of about 200 projectile nucleons undergo N-N interaction, leading to a value of $\langle E_{\text{ZDC}} \rangle$ that is lower than the one of uninteracting Pb ions by a few times (at least) 0.5%. This implies that a precise comparison of the $\langle E_{\text{ZDC}} \rangle$ values for fission events and uninteracting beam might provide some information on the fission mechanism. Indeed in our case such a comparison is rather difficult. This is not due to the resolution of the ZDC (about 7%), since we are averaging E_{ZDC} over a large number of events, but rather to systematic effects. In fact we cannot exclude that the response of the ZDC is different by, say, 1 or 2% for 208 nucleons arranged in a single nucleus (uninteracting Pb ions) or in two fragments of similar mass number (fission events). Therefore, all that can be said is that fission occurs in extremely peripheral collisions, compatible with electromagnetic fission as well as with fission induced by soft nuclear interactions involving very few participant nucleons.

IV. CALCULATIONS

To shed more light on the fission mechanism, the yield of Coulomb fission events expected in our experimental conditions is computed in this section and compared to the measured one. In Sec. IV A are reported the calculations of the Coulomb-fission cross sections for ^{208}Pb and for lighter Pb isotopes. These last are produced by e.m. dissociation of the beam in the thick lead target used in our experiment, as discussed in Sec. IV B. Both the contributions arising from fission of ^{208}Pb and of lighter isotopes are taken into account in Sec. IV C, where the expected yield e.m. fissions is finally evaluated.

A. Coulomb fission cross sections

When two nuclei A and B collide at a given impact parameter b larger than the sum of the nuclear radii (i.e., b

$> b_{\min} \approx R_A + R_B$), the interaction is purely electromagnetic. At high bombarding energy, each nucleus experiences the strong Lorentz-contracted Coulomb field of the other nucleus. According to the Weizsacker-Williams (WW) method [9], this can be expressed in terms of the equivalent virtual photon spectrum $n_B(\omega, b)$, where ω is the energy of the virtual photon. The interaction with nucleus A of a virtual photon (emitted by nucleus B) may lead to its fission and the Coulomb fission cross section for nucleus A is given by

$$\sigma_A^{Cf} = \int_{b \geq b_{\min}} 2\pi b db \int n_B(\omega, b) \sigma_A^{\gamma f}(\omega) d\omega, \quad (1)$$

where $\sigma_A^{\gamma f}(\omega)$ is the photofission cross section of nucleus A . The expression of $n_B(\omega, b)$ can be derived in the frame of classical electromagnetism [10]. For low and high photon energies, the equivalent photon distribution, respectively, approximates to

$$n_B(\omega, b) \approx \frac{Z_B^2}{\pi^2} \frac{\alpha}{\omega b^2} \quad (\omega \ll \gamma/b), \quad (2)$$

$$n_B(\omega, b) \approx \frac{Z_B^2}{2\pi} \frac{\alpha}{\gamma b} e^{-2\omega b/\gamma} \quad (\omega \gg \gamma/b), \quad (3)$$

where α is the fine structure constant, Z_B is the charge number of nucleus B , and γ is the Lorentz factor of nucleus B , taken in the rest frame of nucleus A . These equations show that σ_A^{Cf} increases rapidly with the target nucleus charge ($\sigma_A^{Cf} \propto Z_B^2$) and that at fixed impact parameter, the photon spectrum behaves as $1/\omega$ up to the cutoff energy $\omega_{\text{cut}}(b) = \gamma/b$ and then quickly vanishes. This implies that σ_A^{Cf} increases with the bombarding energy, since more energetic photons are radiated at higher γ .

The cross section σ_{208}^{Cf} for Coulomb fission of ^{208}Pb on a Pb target at 158A GeV can be computed according to Eq. (1). The input for this calculation is the photofission cross section of ^{208}Pb , $\sigma_{208}^{\gamma f}$: data can be found in literature for photon energies ranging from the fission threshold ($\omega = 28$ MeV) up to $\omega = 1$ GeV [15,17]. The calculation is carried out with the following approximations. We use for $n_B(\omega, b)$ the expression (2) up to the cutoff photon energy $\omega_{\text{cut}}(b)$, while for $\omega > \omega_{\text{cut}}(b)$ we put $n_B(\omega, b) = 0$. Moreover, since the maximum photon energy at the SPS is about 2 GeV, the values of $\sigma_{208}^{\gamma f}$ in the region $1 \text{ GeV} < \omega < 2 \text{ GeV}$ are deduced by extrapolating the data previously quoted. Different extrapolations lead to similar values of σ_{208}^{Cf} , of about 380 mb, obtained by using for the minimum impact parameter of Eq. (1) the value $b_{\min} = 15$ fm [33].

The same procedure adopted for ^{208}Pb can be used to compute the e.m. fission cross sections for other nuclei, if the photofission cross sections are known up to sufficiently high photon energies. Unfortunately, this is not the case of Pb isotopes lighter than ^{208}Pb ; nevertheless, we can estimate the e.m. fission cross sections for these nuclei in a different way. Data can be found in literature concerning the photofission cross section for ^{209}Bi [15] up to $\omega = 1$ GeV. Thus, we have computed the Coulomb fission cross section for this nucleus:

it turns out to be about 450 mb for a Pb target at SPS energy, i.e., a value that is very close to the one found for ^{208}Pb . The electro-fission cross sections for ^{207}Pb , ^{206}Pb , and ^{204}Pb have been measured [16] only for electron energies between the fission thresholds and 50 MeV. In this energy interval the cross sections decrease with the isotope mass and lie in a ‘‘corridor’’ delimited by the cross sections for ^{208}Pb (lower bound) and ^{209}Bi (upper bound). If we assume that also at higher photon energies the cross sections for these Pb isotopes still lie in this corridor, we are led to conclude that the values of the Coulomb fission cross sections for these isotopes are between the ones for ^{208}Pb and ^{209}Bi , i.e., between 380 and 450 mb.

B. Thick target effects

In view of computing the expected yield of Coulomb fission events, we have to investigate the effects due to the thick target used in NA50. The ^{208}Pb beam delivered by the SPS impinges on a 12 mm natural lead target. Such a thickness corresponds to about 30% of the nuclear interaction length of Pb projectiles in a Pb target, since the nuclear Pb-Pb cross section is about 7.5 b, leading to $\lambda^{\text{nuc}} \approx 40$ mm. However, beside nuclear interaction, the e.m. one plays also an important role from our point of view, since the cross section $\sigma^{\text{e.m.}}$ for electromagnetic dissociation in Pb-Pb interactions at ultrarelativistic energies turns out to be significantly larger than the nuclear one [10].

The value of $\sigma^{\text{e.m.}}$ for ^{208}Pb can be evaluated according to the WW method, by replacing in integral (1) the photofission cross section with the photon absorption cross section $\sigma_{208}^{\gamma t}$ that is measured up to $\omega = 100$ GeV [10]. We have computed this integral according to the approximations previously adopted for the calculations of the Coulomb fission cross sections and we find $\sigma^{\text{e.m.}} \approx 50$ b, a value that, although slightly larger, is in substantial agreement with the one recently reported in Ref. [34]. Taking into account both nuclear and electromagnetic interaction, we obtain a value of the total (nuclear + e.m.) ^{208}Pb -Pb cross section of about 60 b, corresponding to a total mean free path $\lambda' = 5$ mm for the ^{208}Pb projectiles in a Pb target. Such a value is smaller than the thickness of the NA50 target, so that the probability of finding a ^{208}Pb projectile at a given depth x in the target quickly decreases with x .

At low photon energy (say $\omega < 40$ MeV) the excitation of the giant dipole resonance (GDR) and its subsequent decay, leading to the emission of one or more neutrons, accounts for the largest part of the γ - ^{208}Pb cross section [35]. This implies that Pb isotopes lighter than ^{208}Pb are produced along the target as a consequence of the electromagnetic dissociation of ^{208}Pb in the neutron channel. Since the neutrons are emitted within the angular acceptance of the ZDC, the energy measured by this detector is not affected by such a process, which cannot be identified experimentally. Therefore, as these isotopes are expected to have Coulomb fission cross sections similar to the one of ^{208}Pb , they can contribute as well to the observed Coulomb fission yield.

The isotopic population (i.e., the probability of finding a given projectilelike Pb isotope at a depth x in the target) has been computed analytically, as reported in detail in Ref. [37]. The input for this calculation is represented by the cross-

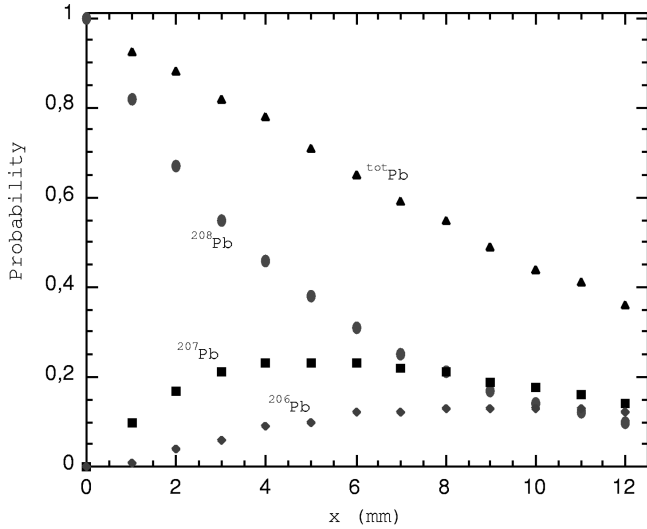


FIG. 6. Probability of finding a ^{206}Pb (diamonds), ^{207}Pb (squares) and ^{208}Pb (circles) as a function of the depth x in the target. The sum of these probabilities [$^{\text{tot}}P(x)$, see text] is also shown (triangles).

sections for e.m. dissociation of lead isotopes in the neutron channel. These have been computed for ^{208}Pb by folding in Eq. (1) the cross sections $^{208}\sigma(\gamma,1n)$ for one and $^{208}\sigma(\gamma,2n)$ for two neutron emission in γ - ^{208}Pb interaction, taken from Ref. [35]. The cross sections that we find for the processes $\text{Pb}(^{208}\text{Pb},^{207}\text{Pb}+n)X$ and $\text{Pb}(^{208}\text{Pb},^{206}\text{Pb}+2n)X$ are, respectively, of about 30 and 5 b, similar to those expected for ^{197}Au - ^{197}Au interactions [36]. Concerning the e.m. dissociation of ^{207}Pb , in our calculation the cross section for the process $\text{Pb}(^{207}\text{Pb},^{206}\text{Pb}+n)X$ has been assumed to be equal to the one for $\text{Pb}(^{208}\text{Pb},^{207}\text{Pb}+n)X$. This is justified by the fact that similar values of $^{207}\sigma(\gamma,1n)$ and $^{208}\sigma(\gamma,1n)$ are reported in literature [35]. The results of the calculation are summarized in Fig. 6, where are shown the probabilities $^{206}p(x)$, $^{207}p(x)$, and $^{208}p(x)$ of finding, respectively, a ^{206}Pb , ^{207}Pb , and ^{208}Pb isotope at a depth x in the target. The probabilities for ^{207}Pb and ^{206}Pb isotopes turn out to be non-negligible, their maximum values being of the order of 25 and 12 %, respectively. The sum $^{\text{tot}}p(x)$ of the probabilities for these three lead isotopes is also shown in the same figure.

C. Expected yield of Coulomb fission events

We are now ready to estimate the relative yield of Coulomb fission events (i.e., the number of fission events per incident Pb ion, as it was defined in Sec. III) that we expect to observe in our experiment. Since, as discussed in Sec. IV A, the cross sections for Coulomb fission are expected to be very similar for ^{206}Pb , ^{207}Pb , and ^{208}Pb , the relative yield of Coulomb fission events is given by

$$n^{Cf}/n_0 = \int_0^{12\text{mm}} ^{\text{tot}}p(x)/\lambda^{Cf} dx, \quad (4)$$

where $\lambda^{Cf} = 815$ mm is the mean free path of lead isotopes for Coulomb fission in a Pb target. This last quantity has been computed by taking for the Coulomb fission cross sec-

tion the value $\sigma_{\text{Pb}}^{Cf} = 380$ mb previously found. The calculation of integral (4) gives $n^{Cf}/n_0 = 0.9 \times 10^{-2}$. This value has to be corrected for the probability of nuclear reinteraction of the fission fragments inside the target, that we have estimated to be about 18%. This leads to an expected yield of fission events per incident Pb ion of about 0.75×10^{-2} , to be compared to the observed one that is $(1.26 \pm 0.16) \times 10^{-2}$.

V. CONCLUSIONS

An exploratory measurement aiming to study the charge of the projectilelike fragments emitted in Pb-Pb interactions at 158A GeV was carried out by placing a Cerenkov detector downstream of the NA50 target. The measurement was performed in parallel with the standard data taking of the experiment, which is devoted to the detection of vector mesons. Therefore, the experimental conditions were optimized for this kind of measurements, where high beam intensities and a thick target are requested, rather than for the study reported here. Nevertheless an evident fission peak was observed in the ADC spectrum of the fragment detector. The amount of energy deposited in the NA50 zero-degree calorimeter indicates that fission occurs in extremely peripheral collisions. In order to clarify the fission mechanism we computed the expected yield of Coulomb fission events in our experimental conditions; it turns out to be 40% smaller than the observed one. This difference could be due to the fact that only the contribution due to ^{208}Pb , ^{207}Pb , and ^{206}Pb was included in the calculation, while the one arising from other lead isotopes and heavy nuclei produced in the target mainly by e.m. interaction was not taken into account. Moreover, fission occurring in materials other than the target could also play a role. In principle, fission due to very peripheral nuclear collisions could also account for such a difference. However, the results of recent high energy experiments with gold and lead beams seem to indicate that the probability of such a process is small.

We hope that in the near future it will be possible to clarify the situation by using a thin lead target to avoid contribution due to fission of nuclei different from ^{208}Pb . Moreover, as the dependence on the target nucleus and on the bombarding energy are expected to be different for fission induced by nuclear and electromagnetic interaction, measurements on lighter target nuclei and at incident energies smaller than 158A GeV, but still in the ultrarelativistic regime, could be useful to identify the fission mechanism. Last but not least, data concerning fission of lead on different target nuclei at bombarding energies close to 1A GeV should be useful to understand the evolution of the fission process as a function of the incident energy.

ACKNOWLEDGMENTS

The technical support provided by G. Alfarone, S. Brasinlin and F. Daudo (INFN Torino) both in the design and in the construction of the fragment detector is acknowledged. One of the authors (E.V.) wishes to thank M. Bernas, P.F. Bortignon, J.C. Hill, A. Molinari, L.G. Moretto, and K.H. Schmidt for fruitful discussions. This work was partially supported by INTAS Grant No. 96-0231.

- [1] V.E. Oberacker, W.T. Pinkston, and H.G.W. Kruse, Rep. Prog. Phys. **48**, 327 (1985).
- [2] M. Eisenbergh and W. Greiner, *Excitation Mechanism of the Nucleus*, 3rd ed. (North-Holland, Amsterdam), Vol. 2, p. 239.
- [3] J. W. Norbury, Phys. Rev. C **43**, R368 (1991).
- [4] M. Justice, Y. Blumenfeld, N. Colonna, D.N. Delis, G. Guarino, K. Hanold, J.C. Meng, J.C. Peaslee, G.F. Wozniack, and L.G. Moretto, Phys. Rev. C **49**, R5 (1994).
- [5] D.E. Greiner, H. Crawford, P.J. Lindstrom, J.M. Kidd, D.L. Olson, W. Schimmerling, and T.J.M. Symons, Phys. Rev. C **31**, 416 (1985).
- [6] Th. Rubehn *et al.*, Z. Phys. A **353**, 197 (1995).
- [7] M. Hesse *et al.*, Z. Phys. A **355**, 69 (1996).
- [8] C.A. Bertulani and G. Baur, Phys. Rep. **163**, 299 (1988).
- [9] E.J. Williams *et al.* Proc. R. Soc. London, Ser. A **139**, 163 (1933); C.F. von Weizsacker, Z. Phys. **88**, 612 (1934); E. Fermi, *ibid.* **29**, 315 (1924).
- [10] M. Vidovic, M. Greiner, and G. Soff, Phys. Rev. C **48**, 2011 (1993).
- [11] G. Bologna, V. Bellini, V. Emma, A.S. Figuera, S. Lo Nigro, C. Milone, and G.S. Pappalardo, Nuovo Cimento A **35**, 91 (1976).
- [12] V. Lucherini *et al.*, Phys. Rev. C **39**, 911 (1989).
- [13] J.B. Martins, E.L. Moreira, O.A.P. Tavares, J.L. Vieira, L. Casano, A. D'Angelo, C. Schaerf, M.L. Terranova, S. Babusci, and B. Girolami, Phys. Rev. C **44**, 354 (1991).
- [14] C. Guaraldo *et al.*, Phys. Rev. C **36**, 1027 (1987).
- [15] L.G. Moretto, R.C. Gatti, S.G. Thompson, J.T. Routti, J.H. Hiesenberg, L.M. Middleman, M.R. Yearian, and R. Hofstadter, Phys. Rev. **179**, 1176 (1969).
- [16] D. Turck, H.G. Clerc, and H. Trager, Phys. Lett. **63B**, 283 (1976).
- [17] J.D.T. Arruda-Neto *et al.*, Phys. Rev. C **41**, 354 (1990).
- [18] B.L. Berman, J.T. Caldwell, E.J. Dowdy, S.S. Dietrich, P. Meyer, and R.A. Alvarez, Phys. Rev. C **34**, 2201 (1986).
- [19] L.G. Moretto, *Proceedings of the Symposium Physics and Chemistry of Fission 1973*, Rochester, N.Y., 1973 (IAEA, Vienna, 1974).
- [20] H.G. Clerc *et al.*, Nucl. Phys. **A590**, 785 (1995).
- [21] A.I. Warwick *et al.*, Phys. Rev. C **27**, 1083 (1983).
- [22] C.J. Waddington and P.S. Freier, Phys. Rev. C **31**, 888 (1985).
- [23] C. Lewenkopf, J. Dreute, A. Abdul-Magd, J. Aichelin, W. Heirich, J. Hufner, G. Rusch, and B. Wiegel, Phys. Rev. C **44**, 1065 (1991).
- [24] C.J. Waddington, Int. J. Mod. Phys. E **2**, 739 (1993).
- [25] M.L. Cherry *et al.*, Phys. Rev. C **52**, 2652 (1995).
- [26] G. Singh and P.L. Jain, Phys. Rev. C **54**, 3185 (1996).
- [27] T. Matsui and H. Satz, Phys. Lett. B **178**, 416 (1986).
- [28] M. Abreu *et al.*, Phys. Lett. B **410**, 327 (1997); M. Abreu *et al.*, *ibid.* **410**, 337 (1997).
- [29] F. Bellaiche, B. Chenis, D. Contardo, O. Drapier, J.Y. Grossiord, A. Guichard, R. Haroutunian, M. Jacquin, F. Ohlsson-Malek, and J.R. Pizzi, Nucl. Instrum. Methods Phys. Res. A **398**, 180 (1997).
- [30] B. Alessandro *et al.*, Nucl. Instrum. Methods Phys. Res. A **360**, 189 (1995).
- [31] R. Arnaldi *et al.*, Nucl. Instrum. Methods Phys. Res. A **411**, 1 (1998).
- [32] Ph. Gorodetzky *et al.*, Nucl. Instrum. Methods Phys. Res. A **361**, 161 (1995).
- [33] C.J. Benesh, B.C. Cook, and J.P. Vary, Phys. Rev. C **40**, 1198 (1989).
- [34] I. Pschenicknov, I.N. Mishustin, J.P. Bondorf, A.S. Botvina, and A.S. Iljinov, Phys. Rev. C **57**, 1920 (1998).
- [35] B.L. Berman and S.C. Fultz, Rev. Mod. Phys. **47**, 713 (1975).
- [36] J.C. Hill, F.H. Wahn, D.D. Schwellembach, and A. R. Smith, Phys. Lett. B **273**, 371 (1991).
- [37] R. Arnaldi, L. Bardi, S. Beolè, N. De Marco, A. Piccotti, and E. Vercellin, NA50 internal note, 1997 (unpublished).